Thermochimica Acta, 199 (1992) 17–24
Elsevier Science Publishers B.V., Amsterdam

Computer coupling of thermodynamics and phase diagrams: the gadolinium–magnesium system as an example [1]

G. Cacciamani, A. Saccone, G. Borzone, S. Delfino and R. Ferro

Istituto di Chimica Generale, Università di Genova, Viale Benedetto XV 3, 16132 Genoa (Italy)

(Received in final form 10 September 1991)

Abstract

A thermodynamic analysis of the binary Gd–Mg system is presented, and its description is optimized using the experimental phase diagram and thermodynamic values. The excess Gibbs energies of the liquid and solid (α-Gd, β-Gd and Mg) solutions were described according to the Redlich–Kister polynomial expansion. The intermediate compounds (GdMg, $GdMg_2$, $GdMg_3$ and $GdMg_5$) were assumed to be stoichiometric phases. A good agreement between the experimental and the computed phase diagram is shown. The results are briefly discussed and compared with those for other binary rare earth–Mg alloys.

INTRODUCTION

Determination of phase equilibria and measurement of thermodynamic properties are often performed separately in alloy chemistry research. Phase diagrams and thermodynamics are strongly correlated, however, and appropriate calculation techniques can be used to optimize the experimental data and to predict the thermodynamic behaviour of a multi-phase system. These techniques are also helpful during the investigation of multi-phase multi-component systems, because they reduce the amount of experimental work by permitting the selection of crucial measurements.

The systematics of R–M alloys (R = rare earth metal, M = a given element) is of particular interest, since the regular and smooth variation of several elemental properties, on passing from one R to the next in the Periodic Table, is a tool for investigation of their influence on alloying behaviour. Moreover, this regular behaviour provides a prediction rule and a reliability criterion in evaluation of data on series of R alloys with the same partner.

Correspondence to: R. Ferro, Istituto di Chimica Generale, Università di Genova, Viale Benedetto XV 3, 16132 Genova, Italy.

[1] Presented at the 12th National Conference on Calorimetry and Thermal Analysis, Bari, Italy, 11–13 December 1990.

TABLE 1

R–Mg phases: stoichiometries, structure types and temperature ranges (K) of stability

Rare earth	Formula (R:Mg)							
	1:1	1:2	1:3	5:24	1:5	5:41	2:17	1:12
La	CsCl < 1018	$MgCu_2$ < 1048	BiF_3 < 1071				Th_2Ni_{17} < 945	$CeMg_{12}$
Ce	CsCl < 984	$MgCu_2$ < 1023	BiF_3 < 1069			Ce_5Mg_{41} < 908	Th_2Ni_{17}	$CeMg_{12}$
Pr	CsCl	$MgCu_2$	BiF_3			Ce_5Mg_{41}		$ThMn_{12}$
Nd	CsCl < 1073	$MgCu_2$ < 1033	BiF_3 < 1053			Ce_5Mg_{41} < 833		
Pm								
Sm	CsCl < 1073	$MgCu_2$ < 1023	BiF_3 < 973		$GdMg_5$ < 838	Ce_5Mg_{41}		
Eu	CsCl	$MgZn_2$			$ErZn_5$		Th_2Ni_{17}	
Gd	CsCl < 1141	$MgCu_2$ < 1029	BiF_3 < 993		$GdMg_5$ < 931			
Tb	CsCl < 1128	$MgZn_2$ < 993	BiF_3 < 878	Ti_5Re_{24} < 828				
Dy	CsCl < 1133	$MgZn_2$ < 983	BiF_3 < 793	Ti_5Re_{24} < 873				
Ho	CsCl < 1118	$MgZn_2$ < 968		Ti_5Re_{24} < 873				
Er	CsCl < 1103	$MgZn_2$ < 943		Ti_5Re_{24} < 873				
Tm	CsCl	$MgZn_2$		Ti_5Re_{24}				
Yb		$MgZn_2$						
Lu	CsCl	$MgZn_2$		Ti_5Re_{24}				

Magnesium alloys are of outstanding technological importance, especially in the aerospace field. Rare earths are of major significance in this connection because they enhance high-temperature properties and improve casting characteristics.

The phase diagrams of several R–Mg systems have been determined: La–Mg [1,2], Ce–Mg [1], Nd–Mg [3], Eu–Mg [4], Sm–Mg [5], Dy–Mg [6], Gd–Mg [2] and Yb–Mg [7]; Tb–Mg, Ho–Mg and Er–Mg are being studied in our laboratory while La–Mg, Ce–Mg, Pr–Mg and Nd–Mg have been assessed in ref. 8. Table 1 summarizes the known R–Mg solid phases, their crystal structures and their melting behaviour.

Data on the thermodynamic properties of R–Mg systems include: vapour pressure measurements of the solid phases at high temperature for several R–Mg systems [9,10], enthalpies of mixing of the Ce–Mg liquid alloys [11], and enthalpies of melting and dissolution in liquid Mg of some Ce–Mg solid phases [11].

EXPERIMENTAL INFORMATION ON THE Gd–Mg SYSTEM

For optimization, all the data are taken into account and weighted to adjust for individual experimental errors. Careful discussion of the literature data is therefore essential. For the phase equilibrium data in particular, it would be helpful if authors were to provide DTA points tables rather than figures only.

Thermal, metallographic and X-ray analyses by Manfrinetti and Gschneidner [2] have shown that the Gd–Mg phase diagram is characterized by four, peritectically melting, intermediate compounds (see also Fig. 1). The solubility of Gd in Mg extends to about 5 at% of Gd, and that of Mg in α-Gd and β-Gd to about 14 and about 36 at% of Mg respectively. Manfrinetti and Gschneidner indicated a temperature error of ± 2 K for the invariant equilibria, and ± 3 K for the points along the liquidus and solidus curves. No composition error is reported for these points, whereas for the eutectic and eutectoid compositions an accuracy of ± 0.5 at% of Mg was estimated. The DTA points used as input data were read from the graph.

The Mg vapour pressure of three solid alloys was measured by Ogren et al. [9] at 710–864 K for Gd–21 at% Mg, at 739–842 K for Gd–32 at% Mg and at 728–900 K for Gd–45 at% Mg. The Mg vapour pressure over a series of Gd–Mg solid alloys was also measured by Pahlman and Smith [10] in the temperature range 650–920 K. They reported $\log(P)$ as a linear function of $1/T$ for several alloys between pure magnesium and Mg–55 at% Gd. The $\log(P_{\text{alloy}}) - \log(P_{\text{Mg}})$ differences at several temperatures were used as input data.

THERMODYNAMIC MODELLING

Optimization requires all the thermodynamic functions of the phases involved to be expressed as analytical functions of temperature and composition, dependent on empirical coefficients that are adjusted to provide the best fitting of the experimental data during the calculation.

The Gibbs energy of the pure elements is described by

$$G(T) = A + BT + CT \ln T + DT^2 + ET^3 + FT^{-1} + GT^7 \qquad (1)$$

The values proposed in ref. 12 (Table 2) were adopted for the $A, \ldots, G$ coefficients. Other thermodynamic functions (H, S, C_p, etc.) can easily be derived from G.

Intermediate compounds were described as stoichiometric in agreement with the phase diagram in ref. 2. Their free energies were expressed as

$$G(x, T) = (1 - x)G_{\text{Gd}}(T) + xG_{\text{Mg}}(T) + A + BT \qquad (2)$$

where A and $-B$ can be interpreted respectively as enthalpies and

TABLE 2

Expansion coefficients used for analytical representation of the Gibbs energy of the pure elements. The column headed "Temperature" indicates the lower limit of the temperature range where the following coefficients are valid [12]

Phase	Temperature (K)	*A*	*B*	*C*	*D*	*E*	*F*	*G*
Gd hcp	200.00	−11600.5250	151.111948	−32.5013000	0.002812650	421363	-1.0812370×10^{-6}	
	1300.00	−8106.1630	115.953605	−27.4590000	−0.000276123		-7.3732500×10^{-7}	
	1535.00	−125618.5110	711.994197	−103.403758	0.015817949	30183452	-6.7254800×10^{-7}	
Gd bcc	298.15	−8028.4400	148.806951	−32.5013000	0.002812650	421363	-1.0812370×10^{-6}	
	1000.00	86879.4860	−747.960507	95.1961984	−0.072542756	−12664161	7.1161570×10^{-6}	
	1535.00	−14097.6260	192.503674	−37.6560000				
	1587.00	−18620.0270	217.622313	−40.9284427	0.000953751	1107440	-4.1967000×10^{-8}	
Gd liquid	298.15	1957.0900	142.499221	−32.5013000	0.002812650	421363	-1.0812370×10^{-6}	
	1000.00	80721.6460	−609.764875	74.8351133	−0.061538012	−10325075	6.0617280×10^{-6}	
	1535.00	−3485.1330	182.116258	−37.1539000				
Mg hcp	298.15	−8367.3400	143.677875	−26.1849782	0.000485800	7895	-1.3936690×10^{-6}	
	923.00	−14130.1850	204.718543	−34.3088000				
Mg liquid	298.15	−165.0970	134.840945	−26.1849782	0.000485800	7895	-1.3936690×10^{-6}	-8.017600×10^{-20}
	923.00	−5439.8690	195.326385	−34.3088000				

TABLE 3

Optimized coefficients (eqns. (2) and (3)) describing the thermodynamic functions of the Gd–Mg phases

Phase	A	B
Liquid	−51294.88	36.86659
	2068.03	3.50768
	−21685.00	10.10016
α-Gd (hcp)	−40966.52	31.49670
β-Gd (bcc)	−46636.27	34.99471
GdMg	−17400.00	8.21492
$GdMg_2$	−19600.00	10.98787
$GdMg_3$	−17000.00	9.44364
$GdMg_5$	−13000.00	7.35641
Mg	−10472.65	4.25257

entropies of formation. However, by analogy with other R–Mg systems, the existence of an appreciable homogeneity range should not be ruled out (especially for the GdMg phase at high temperature).

The excess Gibbs energies of the liquid and solid (α-Gd, β-Gd and Mg) solutions were described according to the Redlich–Kister polynomial expansion [13]

$$G^{E}(x, T) = x_{Gd}x_{Mg}\Sigma_i(A_i + B_iT)(x_{Mg} - x_{Gd})^i \qquad (3)$$

with $i = 0, \ldots, 2$ for the liquid and $i = 0$ for the solid solutions.

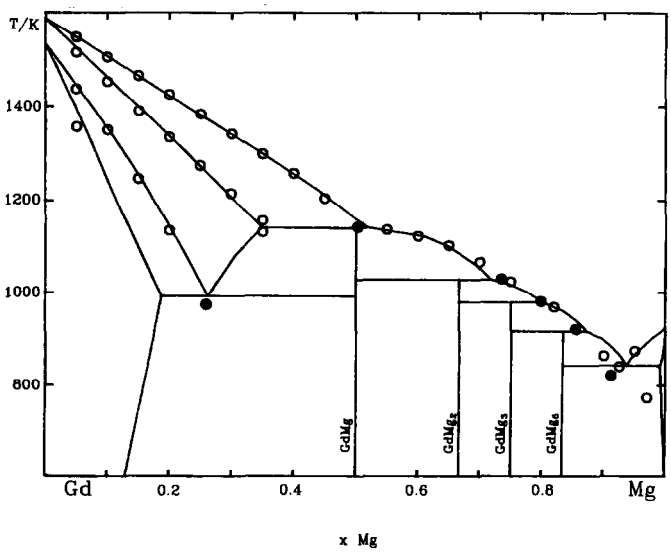

Fig. 1. Gd–Mg system: comparison between the computed phase diagram (continuous line) and the experimental points [2]. ○ two phase equilibria; ● invariant equilibria.

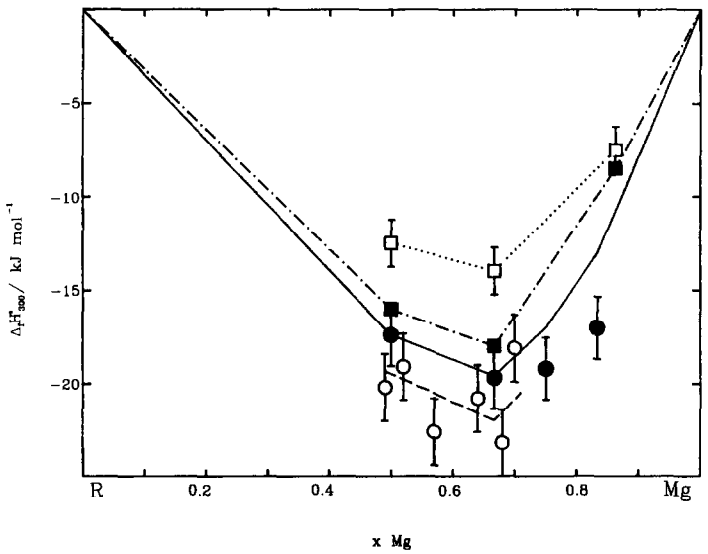

Fig. 2. Calculated $\Delta_f H°$ of the Gd–Mg solid alloys (solid line) compared with the $\Delta_f H°$ of some similar systems: ○, Sm–Mg system, calorimetric data (this work, preliminary); ●, Gd–Mg system, from vapour pressure measurements [10]; □, Y–Mg system, from acid solution calorimetry [15]; ■, Y–Mg system, computed [16].

SYSTEM OPTIMIZATION

The Gd–Mg system was optimized with the computer program prepared by Lukas [14]. This first uses a least-squares method to calculate the

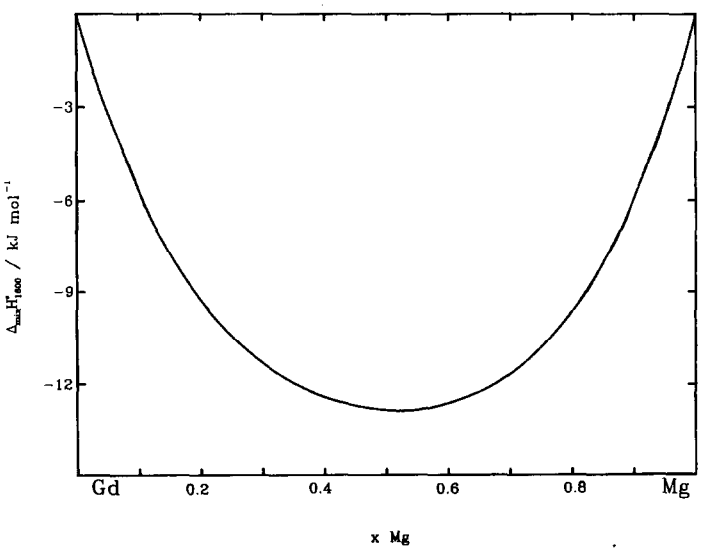

Fig. 3. Gd–Mg liquid alloys: computed values of $\Delta_{mix}H°$.

unknown coefficients from experimental data taking their uncertainty into account. It then determines the computed versions of the phase diagram and the thermodynamic functions.

The coefficients are listed in Table 3. The computed phase diagram is compared with the input data in Fig. 1.

Figures 2 and 3 represent a prediction of the trends of the enthalpies of formation of the solid phases and the mixing enthalpy of the liquid.

DISCUSSION

Very good agreement between the computed phase diagram and the experimental points from ref. 2 was found (Fig. 1 and Table 4) with small differences (a few K or at%) only for the Mg-rich eutectic and for the solid solubility of Gd in Mg, which are attributable either to an inadequate thermodynamic phase description (especially the Mg solid solution) or to possible errors due to metastable situations, such as those observed in the Mg-rich portions of several R–Mg systems.

The literature offers very few data on assessment of the thermodynamic properties of solid intermediate compounds. The $\Delta_f H°$ of the solid phases calculated in [10] at relatively high temperature were therefore taken as the starting values and adjusted by trial and error. The trend of these final values is compared in Fig. 2 with experimental and computed data for similar systems. Those for Sm–Mg alloys have been determined calorimetrically in our laboratory, while those for the Y–Mg system include some obtained calorimetrically in [15] and others computed in [16] while optimizing the diagram. A fair agreement is observed. It can be seen that the values proposed for Gd–Mg alloys are intermediate between those reported for the Sm–Mg and Y–Mg alloys. This fits the general trend observed for R alloys.

The values computed for the $\Delta_{mix} H°$ values in the liquid state are shown in Fig. 3. No experimental data are available for Gd or its neighbouring

TABLE 4

Gd–Mg invariant equilibria: comparison between experimental and computed temperatures

Equilibrium	Temperature (K)	
	Experimental	Computed
β-Gd $\rightleftharpoons$ α-Gd + GdMg	973	991
β-Gd + liquid $\rightleftharpoons$ GdMg	1141	1140
GdMg + liquid $\rightleftharpoons$ $GdMg_2$	1029	1028
$GdMg_2$ + liquid $\rightleftharpoons$ $GdMg_3$	980	979
$GdMg_3$ + liquid $\rightleftharpoons$ $GdMg_5$	920	915
liquid $\rightleftharpoons$ $GdMg_5$ + Mg	821	842

R–Mg alloys. Comparison with those reported for Ce–Mg alloys shows a satisfactory concordance.

REFERENCES

1 R. Vogel and T. Heumann, Z. Metallkd., 38 (1947) 1.
2 P. Manfrinetti and K.A. Gschneidner, Jr., J. Less-Common Met., 123 (1986) 267.
3 S. Delfino, A. Saccone and R. Ferro, Metall. Trans. A, 21A (1990) 2109.
4 W. Muhlpfordt and W. Klemm, J. Less-Common Met., 17 (1969) 127.
5 A. Saccone, S. Delfino, G. Borzone and R. Ferro, J. Less-Common Met., 154 (1989) 47.
6 A. Saccone, S. Delfino, D. Maccio', R. Ferro, Z. Metallkd., 82 (1991) 568.
7 O.D. McMasters and K.A. Gschneidner, Jr., J. Less-Common Met., 8 (1965) 289.
8 A.A. Nayeb-Hashemi and J.B. Clark, Bull. Alloy Phase Diagrams, 9 (1988) 162.
9 J.R. Ogren, N.J. Magnani and J.F. Smith, Trans. Metall. Soc. AIME, 239 (1967) 766.
10 J.E. Pahlman and J.F. Smith, Metall. Trans., 3 (1972) 2423.
11 K. Nagarajan and F. Sommer, J. Less-Common Met., 142 (1988) 319.
12 A.T. Dinsdale, SGTE data for pure elements, NPL Rep. DMA(A) 195, September 1989.
13 O. Redlich and A.T. Kister, Ind. Eng. Chem., 40 (1948) 345.
14 H.L. Lukas, J. Weiss and E.Th. Henig, CALPHAD, 6 (1982) 229.
15 J.F. Smith, D.M. Bailey, D.B. Novotny and J.E. Davison, Acta Metall., 13 (1965) 889.
16 Q. Ran, H.L. Lukas, G. Effenberg and G. Petzow, CALPHAD, 12 (1988) 375.